

Ronald J. Parise  
PARISE RESEARCH TECHNOLOGIES

G. F. Jones  
Brett Strayer  
Villanova University

#### ABSTRACT

Thermoelectric generators (TEGs) are solid state devices that convert thermal energy into electrical energy. Using the nighttime sky, or deep space, with an effective temperature of 4°K as a cold sink, the TEG module presented here can produce electrical power at night. The "hot" junction is supplied energy by the ambient air temperature or some other warm temperature source. The cold junction of the TEG is insulated from the surroundings by a vacuum cell, called a Vacuum Pod™ improving its overall effectiveness.

Studies have shown that with particular TEG module designs, a temperature differential across the TEG can be achieved that will produce an estimated 10mW/cm<sup>2</sup>. This is comparable to the energy available from photovoltaic cells in the noontime sun. Therefore a prototype Nighttime Solar Cell™ is being built and will be tested to determine the effectiveness of the cold junction insulator as well as the influence of other system parameters.

The prototype TEG module is being built with off-the-shelf components to reduce cost and emphasize the availability of standard materials. The prototype is currently in the manufacturing stage.

The theoretical results of the model presented here indicate that the vacuum cell is a very effective addition for the efficient production of electrical energy for TEG modules in a terrestrial application.

#### INTRODUCTION

The Nighttime Solar Cell™ is a device that utilizes a thermoelectric-photovoltaic (TEPV) cell to generate electrical energy both day and night in a terrestrial application [1]. The unique vacuum cell design of the TEPV module isolates the cold junction of the thermoelectric generator (TEG) from the surroundings but provides an unobstructed view of deep space. The TEG utilizes deep space as a thermal sink with an effective temperature of 4°K [2]. Much work has been accomplished using deep space as a thermal sink for cooling in orbiting spacecraft applications [3] as well as in terrestrial building uses [4, 5, 6]. Reduced pressure assemblies in solar panels have also been utilized [7] to eliminate the natural convection currents to improve

system performance. In the present application of deep space as a thermal sink, the hot junction of the TEG is supplied energy from the ambient air.

A prototype cell is currently being manufactured to determine the effectiveness of deep space as a thermal sink in the operation of the TEGs. Initial prototype design will use only TEGs for the production of electrical energy. The thermal analysis presented here is a first step to predict the temperature differences the prototype will experience with the information used in the initial phase of prototype design. TEG module design optimization is discussed at length in several references [8, 9], and will be utilized extensively in the second phase of module development in the design of the next prototype. The critical design parameters for electrical operation of the TEG are the temperature differences (voltage) and the electrical resistance (current). As the model matures and data is collected from the first prototype, the thermal model will be utilized as a design tool for future TEG module designs.

#### MODELING APPROACH

A quasi one-dimensional, steady-state thermal model is developed to determine the temperature differential between the hot and cold junctions of the TEG. A quasi one-dimensional approach is used because the thermal conductivity of the TEG elements (bismuth telluride,  $k=1.5$  W/mK) is much less than the material used for lateral conduction (copper,  $k=400$  W/mK). An order of magnitude analysis shows the thermal conductance in the axial direction can be up to three orders of magnitude less than the conductance in the lateral direction. Therefore initial design considerations dictate a one-dimensional model.

Figure 1 shows the configuration of the physical parameters utilized in the model. The thermal source supplies energy to the module at  $T_{\infty}$ . There may be a convection (as well as radiation) boundary condition at the hot plate of the TEG module, where  $h_b$  is the convective heat transfer coefficient. However, in this first application, modes of energy transfer to the hot plate are neglected and the hot junctions are assumed to be at constant temperature  $T_h$ . The energy travels through the TEG elements (the p-n material), through the cold junctions into the cold junction plate (CJP). The surface of the CJP is assumed to be a gray, diffuse surface

with  $\epsilon_c = \alpha_c$  at temperature  $T_c$ . The surface facing the nighttime sky is treated to have an emissivity  $\epsilon_c$  of 0.96. The CJP then radiates thermal energy to deep space through the window covering the aperture of the vacuum cell.

Deep space is modeled as a black body at temperature  $T_s = 4^\circ\text{K}$ . Initial model development will have a three-band radiation capability for energy transmission through the window. The two wavelengths that separate the three bands are cutoff wavelengths  $\lambda_1$  and  $\lambda_u$ . The radiation surface properties, for absorptivity ( $\alpha$ ), reflectivity ( $\rho$ ), and transmissivity ( $\tau$ ), are given subscripts 1, 2, and 3 to designate their values in each of the three bands. In any band, emissivity and absorptivity are assumed to be equal,  $\epsilon = \alpha$ . Initial model results will use a single band between  $8\mu\text{m}$  and  $13\mu\text{m}$  where approximately one-third of the total radiative energy spectrum is transmitted. All radiative view factors are assumed to be one.

The exterior of the window is exposed to the ambient temperature,  $T_\infty$ , through a specified heat transfer coefficient,  $h_w$ . Temperature variations through the window are neglected.

The thermoelectric properties of the Seebeck ( $S_{ab}$ ) and Peltier ( $\Pi_{ab}$ ) coefficients, thermal conductivity ( $k$ ), and the electrical resistivity ( $R'$ ) are assumed to be constant. The length of the thermoelectric elements in the direction of heat flow is  $L$ .

The effect of increasing the heat transfer surface of the CJP will be investigated relative to the thermal conductive area of the thermoelectric elements. Therefore the ratio of the CJP radiative area to the TEG conduction area is designated as  $A_r$  and is an adjustable parameter. The CJP area then becomes a fin utilized to enhance radiative heat transfer with deep space. Initially the fin effectiveness in all directions will be assumed one.

#### EQUATION DEVELOPMENT

##### Radiation Model

The heat flow rate  $Q_c$  passing through the thermoelectric elements to the CJP and into deep space may be expressed as an energy balance on the cold junction plate, accounting for thermal emission and the radiosity  $J_c$ . The heat flux that results from this heat flow rate is  $q_c = Q_c/A_w$ , where  $A_w$  is the area of the window (also taken to be the area of the cold plate). The flux  $q_c$  is written as

$$q_c = \frac{\epsilon_c}{1 - \epsilon_c} [\sigma T_c^4 - J_c]. \quad (1)$$

The heat flux  $q_c$  may also be written as  $J_c - G_c$ , where  $G_c$  is

the irradiation incident on the cold plate.  $G_c$  comes from three sources: the fraction of energy from the night sky that is transmitted through the window, emission from the window, and the fraction of  $J_c$  that is reflected from the window. Thus

$$q_c = (1 - \rho_w)J_c - \tau_w \sigma T_s^4 - \epsilon_w \sigma T_w^4. \quad (2)$$

An energy balance on the window accounts for the convective heat transfer rate at the external surface of the window and the net radiative energy it absorbs. Thus

$$h_w(T_\infty - T_w) = 2\epsilon_w \sigma T_w^4 - \epsilon_w \sigma T_s^4 - \epsilon_w \sigma T_w^4. \quad (3)$$

All radiative properties in eqns. (2) and (3) are written as the sum of three contributions from their respective bands. For example,  $\epsilon_w$  in the term  $\epsilon_w \sigma T_s^4$  in eqn. (3) may be written as

$$\epsilon_w = \epsilon_1 F(0, \lambda_1 T_s) + \epsilon_2 F(\lambda_1 T_s, \lambda_u T_s) + \epsilon_3 F(\lambda_u T_s, \infty), \quad (4)$$

where  $F(x, y)$  is the blackbody emissive power fraction over the band of  $\lambda T$  defined by the values of the first ( $x$ ) and second ( $y$ ) arguments in  $F(x, y)$  [10]. In eqns. (2) and (3), the radiation properties of  $J_c$  are based on the band model at temperature  $T_c$ .

##### Heat Conduction Model

A steady-state, quasi one-dimensional heat conduction model with internal energy generation is used. One boundary condition is the radiative heat flux ( $q_c$ ) at the cold plate, where  $q_c$  is based on the surface area  $A_w$  and the temperature of deep space,  $4^\circ\text{K}$ . The second boundary condition is convection heat transfer at the hot junction plate. Here, the thermal source temperature is  $T_\infty$  where the heat transfer coefficient is  $h_b$ .

The area for heat conduction in the individual thermoelectric elements is  $A_e$ . The area ratio,  $A_r$ , is equal to  $A_w/A_e$ . This is the area parameter used in the development of the conduction model, where  $A_r$  is greater than 1.

From this information, the temperature distribution in the thermoelectric elements may be written as

$$T_t(\eta) = -\phi \eta^2 / 2 - Bi \eta T_\infty + (\phi / Bi + T_\infty - q_c / h_b)(1 + Bi \eta), \quad (5)$$

where  $Bi$  is the Biot number,  $A_r h_b L / k$ ;  $\phi$  is the energy generation parameter,  $q'' L^2 / k$ , where  $q''$  is the rate of energy generation per unit volume; and  $\eta$  is the dimensionless local coordinate,  $x/L$ .

There is a need to relate the term  $q''$  in the energy generation parameter to the junction temperatures,  $T_h$  or  $T_c$ . The electric current flowing through the thermoelectric elements is based on the Seebeck coefficients,



$$i_{ab} = -q_c A_w / [T_c (S_p - S_n)]. \quad (6)$$

The rate of energy generation per unit volume is

$$q''' = i_{ab}^2 R / A_c^2. \quad (7)$$

Combining these two equations to eliminate the current, an expression is obtained for  $\phi$  as

$$\phi = \{A_c q_c L / [(T_c (S_p - S_n))]^2 R / k\}. \quad (8)$$

The cold and hot plate temperatures,  $T_c$  and  $T_h$ , are

$$T_c = T_c(\phi = 1), \text{ and } T_h = T_c(\phi = 0). \quad (9)$$

Finally, the overall heat transfer coefficient for the hot junction may be written as

$$h_{b,v} = h_b + \frac{\sigma(T_\infty^2 + T_h^2)(T_\infty + T_h)}{2\epsilon_b - 1}, \quad (10)$$

where  $h_{b,v}$  is the combined heat transfer coefficient due to convection and radiation. In this expression, the thermal source may provide energy to the hot junction plate through convection and radiation heat transfer.

#### SOLUTION

The sophistication of the thermal model exceeds the initial requirements for the design of the first prototype. Therefore the model to predict the temperature difference between the hot and cold junctions of the TEGs is simplified as follows. The hot junction plate is maintained at a constant temperature  $T_h$ . Internal energy generation is considered negligible. All radiative interactions occur between the black sky and the surface of the CJP only.

The TEG elements modeled are p- and n-doped bismuth telluride with an area  $A_c$  of  $1\text{mm}^2$  and length  $L$  of 2mm. These were standard element sizes available from suppliers. The thermal model uses a two-element configuration to determine the temperature differential  $\Delta T = T_h - T_c$  of the paired junction. Figure 2 shows the effect on the temperature difference across the elements when the area ratio increases. The amount of energy transferred to deep space increases significantly as the CJP area increases, providing a large thermal driving force. The ratio between the CJP area and the elements area will be maximized within the physical limitations of the module and window area.

In Figure 3, increasing the temperature of the hot junction plate in the normal range of expected ambient temperatures has little effect on the temperature difference across the

elements. Therefore, unless a source of high temperature energy is available to drive the TEGs, not much electrical energy will be available from the module.

Figure 4 illustrates the effect of the thermal conductance,  $K_{TE} = kA_c/L$ , on the temperature difference  $\Delta T$  across the TEG elements. The influence of two physical parameters,  $A_c$  and  $L$ , can be selected to increase module performance significantly. Increasing the length of the elements and/or reducing their area are very controllable dimensions in the manufacture of the elements. These two parameters will be explored extensively in the building of the prototype to maximize cell performance.

#### DISCUSSION

The most dramatic change in the temperature difference between the hot and cold plates is with respect to the area ratio. Practical concerns will limit the size of the CJP area. The thermal conductance can also be used to improve the thermal performance of the module by increasing the length of the elements or reducing the cross-sectional area. Again, this will be within the practical confines of the module. The temperature of the thermal source has very little effect on the temperature difference in the normal operating range of expected ambient temperatures.

#### CONCLUSIONS

The thermal model performed well in predicting the temperature difference between the hot and cold junctions of the TEGs. The significant influence of the area ratio and the thermal conductance provide parametric guidelines for the design of the prototype Nighttime Solar Cell™. The performance of the cell can improve with a marked decrease in the thermal conductance by reducing the thermal conductivity of the p-n material, that is, using a material other than the bismuth telluride. Material development in this area would contribute greatly to the operation of the module.

#### CONTACT

For information on the Nighttime Solar Cell™, please contact Ronald J. Parise, President, PARISE RESEARCH TECHNOLOGIES, 101 Wendover Road, Suffield, CT 06078.

#### REFERENCES

1. Parise, Ronald J., Nighttime Solar Cell™, IECEC98, Colorado Springs, CO, 1998, Paper No. IECEC-98-133.

2. Bliss, Raymond W., Jr., Atmospheric Radiation Near the Surface of the Ground: A Summary for Engineers, Solar Energy, Vol. 5, p103, (1961).
3. Annable, R. V., Radiant Cooling, Applied Optics, Vol. 9, No. 1, p185, (1970).
4. Kimball, B.A., Cooling Performance and Efficiency of Night Sky Radiators, Solar Energy, Vol. 34, No. 1, p19, (1985).
5. Ali, A. Hamza H., Taha, I.M.S., and Ismail, I.M., Cooling of Water Flowing Through a Night Sky Radiator, Solar Energy, Vol. 55, No.4, p235, (1995).
6. Hirano, Sastoshi and Saitoh, Takeo S., IECEC98, Colorado Springs, CO, 1998, Paper No. IECEC-98-369.
7. Eaton, C.B. and Blum, H.A., The Use of Moderate Vacuum Environments as a Means of Increasing the Collection Efficiencies and Operating Temperatures of Flat-Plate Solar Collectors, Solar Energy, Vol. 17, p151, (1975).
8. Culp, Archie W., Jr., Principles of Energy Conversion, McGraw-Hill Book Company, New York, NY, 1979.
9. Angrist, Stanley W., Direct Energy Conversion, Fourth Edition, Allyn and Bacon, Inc., Boston, Massachusetts, 1982.
10. Dunkle, R.V., Thermal Radiation Tables and Applications, Transaction of the ASME, Paper No. 53-A-220, 1953.

DEEP SPACE @ 4 K,  $T_s$

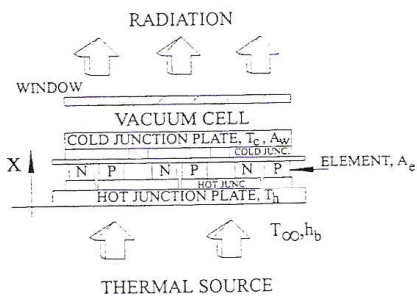


Figure 1. Model Configuration.

SOLAR

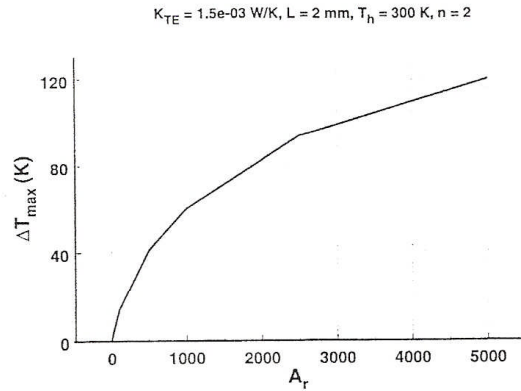


Figure 2. Temperature Differential  $\Delta T$  versus area ratio  $A_r$ .

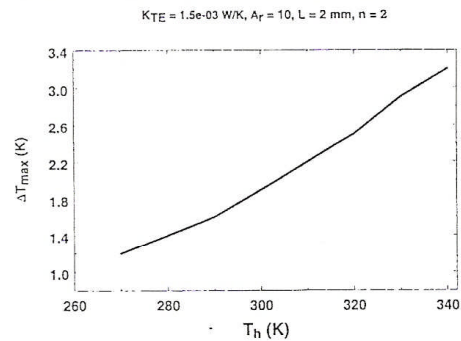


Figure 3. Temperature Differential  $\Delta T$  versus source Temperature  $T_h$ .

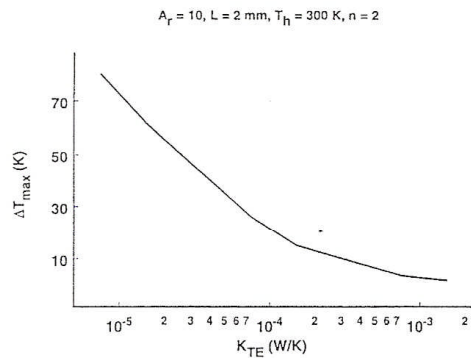


Figure 4. Temperature Differential  $\Delta T$  versus thermal conductance  $K_{TE} = k_{TE}A_e/L$ .